

# The syntheses, characterization and properties of some metallophthalocyanine complexes substituted by (*N*-(2-hydroxyethyl)piperazine)-*N'*-2-ethane sulfonic acid (HEPES)

Ziyang Huang<sup>a,b</sup>, Jiandong Huang<sup>a</sup>, Naisheng Chen<sup>a</sup>, Jinling Huang<sup>a,\*</sup>

<sup>a</sup> Institute of Research on Functional Materials, Fuzhou University, Fuzhou 350002, China

<sup>b</sup> College of Chemistry and Materials Science, Fujian Normal University, Fuzhou 350007, China

Received 19 March 2007; received in revised form 16 August 2007; accepted 19 August 2007

Available online 2 September 2007

## Abstract

Eight novel piperazine derivatives of metal (Zn, Co, Ni, Cu) phthalocyanine complexes were synthesized from two precursors obtained by the nucleophilic substitution of (*N*-(2-hydroxyethyl)piperazine)-*N'*-2-ethane sulfonic acid (HEPES) with both 3-nitro-phthalonitrile and 4-nitro-phthalonitrile. The complexes are characterized by IR, elemental analysis, <sup>1</sup>H NMR and mass spectroscopy; the UV–vis absorption spectra, rate of singlet oxygen yields, fluorescence spectra and quantum yields of the compounds are discussed.

© 2007 Published by Elsevier Ltd.

**Keywords:** Phthalocyanine; HEPES; Synthesis; Property; UV–vis spectrum; Solubility

## 1. Introduction

For many years, phthalocyanines (Pcs) have attracted much attention in some research fields such as chemical sensor, optical information storage material, liquid crystal display device, and low order conductivity material as well as photosensitizer for photodynamic therapy (PDT), and so on [1,2]. As the second generation photosensitizers for PDT in the treatment of cancer, phthalocyanines, particularly the zinc and aluminum derivatives, are the mostly studied [3–6]. Due to their difficulty to be dissolved, the unsubstituted zinc phthalocyanine is utilized only in liposomal form, showing with certain PDT activity [3]. In order to enhance the water solubility of Pcs, some polar derivatives such as sulfonated, amino and hydroxy derivatives have received attention. Although some of these Pcs such as ZnPc-liposome [3], AlPcS<sub>4</sub> (aluminum phthalocyanine tetrasulfonate) [4], Pc 4 (HOSiPc–OSi(CH<sub>3</sub>)<sub>2</sub>(CH<sub>2</sub>)<sub>3</sub>N(CH<sub>3</sub>)<sub>2</sub>) [5], and di-sulfonated

di-phthalimidomethyl phthalocyanine zinc (ZnPcS<sub>2</sub>P<sub>2</sub>) [6] show good PDT behavior and low phototoxicity in animal body trial, they are still in need of finding widespread acceptance in clinic.

Owing to the biological effects of (*N*-(2-hydroxyethyl)piperazine)-*N'*-2-ethane-sulfonic acid (HEPES) indicated in literature [7], we have designed and synthesized several phthalocyanines substituted by HEPES in order to find new properties and better biological activities, which will be used for special fields and expected to be used in PDT. Synthetic routes to metal phthalocyanine complexes involve the initial synthesis of phthalonitrile precursors, followed by cyclization in the presence of metal salts so as to form the phthalocyanine from precursors. Eight new piperazine derivatives of metal (Zn, Co, Ni, Cu) phthalocyanine complexes both in  $\alpha$ -position and  $\beta$ -position were synthesized and characterized. The results show that these complexes possess good solubility in organic polar solvents, and the UV–vis absorption spectra, rate of singlet oxygen yield, fluorescence spectra and quantum yields are examined. Besides, the experimental study on bioactivity of these complexes will be explored.

\* Corresponding author. Tel./fax: +86 591 8370 9114.

E-mail address: [hjl@fzu.edu.cn](mailto:hjl@fzu.edu.cn) (J. Huang).

## 2. Experimental

### 2.1. Materials

*N,N'*-Dimethylformamide (DMF) and *n*-pentanol were freshly distilled under vacuum after pretreatment in 4 Å molecular sieve for 24 h. Anhydrous potassium carbonate and anhydrous zinc acetate were dried at 103 °C for 12 h. Anhydrous nickel chloride and anhydrous cobalt chloride were prepared as described in literature [8]. All reagents were purchased from Sinopharm Chemical Reagent Co., Ltd., except HEPES and 1,3-diphenylbenzotriazole (DPBF) was purchased from Alfa Aesar, 100–120 mesh ZCX-II type column chromatography silica gel purchased from Qingdao Haiyang Chemical Co., Ltd., 1,8-diaza-bicyclo[5.4.0]undec-7-ene (DBU) purchased from Aldrich, and Cremophor EL, a castor oil derivative purchased from Sigma, which were used without further purification.

### 2.2. Equipments

Infrared spectra were recorded on a Perkin–Elmer FT-IR spectrometer in Fuzhou University, using potassium bromide pellets of solids. <sup>1</sup>H NMR spectra with DMSO-*d*<sub>6</sub> as solvent and TMS (tetramethylsilane) as the internal standard were recorded on Varian Unity 500 NMR. Mass spectra were recorded on a Finnigan LCQ Deca Xp Max, Thermo Electron Corporation. Elemental analyses were carried out on a Vario EL III Elementar run by the Fujian Institute of Research on the Structure of Matters. UV–vis spectra were recorded on a Perkin–Elmer Lambda 800 UV–VIS spectrometer. Melting point was measured by a YRT-3 melting point meter made in P.I.T., Tianjin University. Laser (670 nm) was generated from a PDT 670 nm Laser Meter. Fluorescence emission spectra and quantum yield were recorded on a FL/FS920 TCSPC Lifetime Spectrometer and Spectrofluorimeter.

### 2.3. Syntheses of phthalocyanine precursors

#### 2.3.1. Synthesis of 2-(4-(2-(2,3-dicyanophenoxy)ethyl)piperazin-1-yl)ethane sulfonic acid (**3**)

HEPES (357 mg, 1.5 mmol) was added to a mixture of 3-nitro-phthalonitrile (520 mg, 3.0 mmol), anhydrous potassium carbonate (828 mg, 6.0 mmol) and 30 ml DMF at room temperature, nitrogen gas was bubbled. The reaction mixture was stirred at 80 °C for 24 h, and then distilled to remove DMF under reduced pressure, 30 ml KOH (0.10 mol/L) was added to dissolve mixture, the insoluble precipitate was removed by membrane filter. Then HCl (2.0 mol/L) was added to the solution to adjust pH to 3–4, the solution was filtered, residue was dried at 70 °C for 12 h. After ethyl acetate (40 ml) was added for dissolving residue, the solution was purified by column chromatography on silica gel (a 100–120 mesh ZCX-II type column chromatography silica gel purchased from Qingdao Haiyang Chemical Co., Ltd.) with ethyl acetate as eluent; a light yellow solid was obtained after distilled to remove ethyl acetate and dried at 70 °C for 24 h; the reaction

is shown in Fig. 1a. Compound **3**: yield 46%, m.p. 177.3–179.2 °C. Elem. Anal. Calcd. for C<sub>16</sub>H<sub>20</sub>N<sub>4</sub>O<sub>4</sub>S: C, 52.73%; N, 15.37%; H, 5.53%. Found: C, 52.68%; N, 15.35%; H, 5.60%. IR (KBr,  $\nu_{\max}/\text{cm}^{-1}$ ): 3234 (SO<sub>3</sub>–H), 2254, 2230 (C≡N), 1586, 1174 (Ar skeleton), 1467 (CH<sub>2</sub>), 1353 (C–S), 1317 (C–N). <sup>1</sup>H NMR (DMSO-*d*<sub>6</sub>,  $\delta$  (ppm)): 3.00 (2H, CH<sub>2</sub>), 3.16 (2H, CH<sub>2</sub>), 3.71 (2H, CH<sub>2</sub>), 3.89 (2H, CH<sub>2</sub>), 7.37 (1H, Ar-H<sub>3</sub>), 7.53 (1H, Ar-H<sub>5</sub>), 7.70 (1H, Ar-H<sub>6</sub>), 12.04 (1H, SO<sub>3</sub>–H). MS (*m/z*): 364 (M<sup>+</sup>), 366 ([M + 2H]<sup>+</sup>).

#### 2.3.2. Synthesis of 2-(4-(2-(3,4-dicyanophenoxy)ethyl)piperazin-1-yl)ethane sulfonic acid (**4**)

HEPES (357 mg, 1.5 mmol) was added to a mixture of 4-nitro-phthalonitrile (390 mg, 2.3 mmol), anhydrous potassium carbonate (828 mg, 6.0 mmol) and 23 ml DMF at room temperature, nitrogen gas was bubbled. The reaction mixture was stirred at 50 °C for 72 h, and then distilled to remove DMF in vacuum system, 30 ml KOH (0.10 mol/L) was added to the reaction mixture for dissolving residue, the insoluble precipitate was removed by membrane filter. Then 1.0 mol/L HCl was added to solution to adjust pH to 3–4, the solution was extracted by 50 ml ethyl acetate three times, distilled to remove ethyl acetate, residue was dried at 70 °C for 12 h. After 40 ml toluene/acetone = 3:1 (v/v) was added for dissolving residue, the solution was purified by column chromatography on silica gel with toluene/acetone = 3:1 (v/v) as eluent; a light yellow solid was obtained after distillation to remove solvent and dried at 70 °C for 24 h, the reaction is shown in Fig. 1b. Compound **4**: yield 38%, m.p. 203.6–205.4 °C. Elem. Anal. Calcd. for C<sub>16</sub>H<sub>20</sub>N<sub>4</sub>O<sub>4</sub>S: C, 52.73%; N, 15.37%; H, 5.53%. Found: C, 52.64%; N, 15.34%; H, 5.63%. IR (KBr,  $\nu_{\max}/\text{cm}^{-1}$ ): 3268 (SO<sub>3</sub>–H), 2243 (C≡N), 1604, 1567 (Ar skeleton), 1495 (CH<sub>2</sub>), 1344 (C–S), 1313 (C–N), 1227 (Ar–O). <sup>1</sup>H NMR (DMSO-*d*<sub>6</sub>,  $\delta$  (ppm)): 2.94 (2H, CH<sub>2</sub>), 3.10 (2H, CH<sub>2</sub>), 3.70 (2H, CH<sub>2</sub>), 3.88 (2H, CH<sub>2</sub>), 7.22 (1H, Ar-H<sub>3</sub>), 7.41 (1H, Ar-H<sub>5</sub>), 7.92 (1H, Ar-H<sub>6</sub>), 11.48 (1H, SO<sub>3</sub>–H). MS (*m/z*): 364 (M<sup>+</sup>).

### 2.4. Syntheses of metallophthalocyanine complexes

#### 2.4.1. 1,8(11),15(18),22(25)-Tetra-[2-[4-(2-sulfoethyl)piperazin-1-yl]ethoxy]phthalocyanine zinc (**3a**)

A mixture of **3** (182 mg, 0.50 mmol), anhydrous zinc acetate (50 mg, >0.125 mmol), and 6.0 ml *n*-pentanol as solvent was heated to 70 °C and nitrogen gas was bubbled, then 0.20 ml DBU as catalyst was added. The mixture was heated to 150 °C quickly with stirring and refluxing at 150 °C for 6–8 h, the mixture had transformed to dark green eventually. Next, *n*-pentanol was evaporated in vacuum system, 50 ml KOH (0.20 mol/L) was added to transform product into potassium salt, the solution was filtered after 30 min stirring, HCl (2.0 mol/L) was added to adjust filtrate pH to 2, the solution was filtered after 30 min aging, residue was obtained after washing with water and dried at 100 °C for 12 h. The reaction is shown in Fig. 1a.

DMF/CH<sub>3</sub>OH = 1:1 (v/v, 25 ml) was added to dissolve the residue, the solution was purified by column chromatography

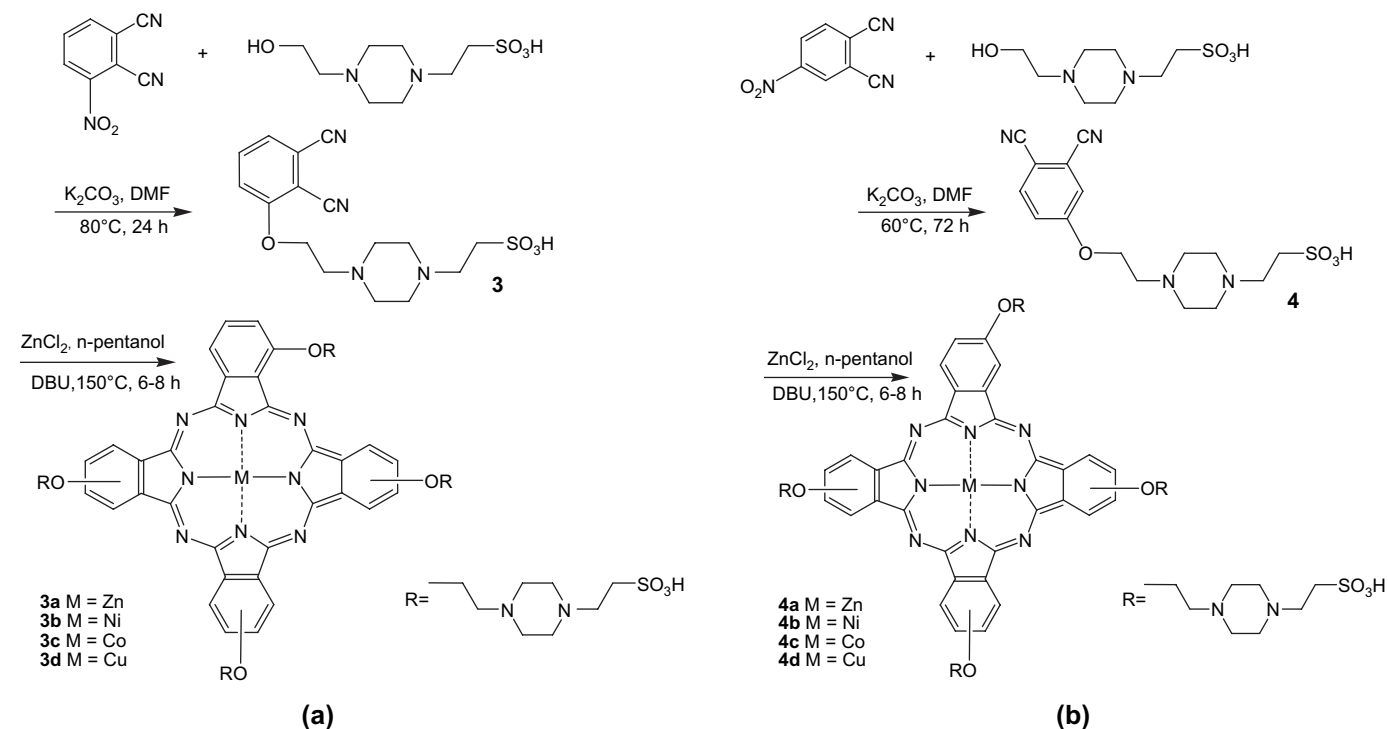


Fig. 1. Synthetic routes of the title complexes.

on silica gel with DMF/CH<sub>3</sub>OH = 1:1 (v/v) as eluent (1), a green solid was obtained after distillation to remove solvent and dried at 110 °C for 12 h. Then 30 ml ethyl acetate was added to dissolve the green solid, the solution was purified by column chromatography on silica gel with ethyl acetate as eluent (2), **3a** was obtained after distillation to remove the solvent and dried at 110 °C for 24 h. Compound **3a**: yield 28.1%. Elem. Anal. Calcd. for C<sub>64</sub>H<sub>80</sub>N<sub>16</sub>O<sub>16</sub>S<sub>4</sub>Zn: C, 50.47%; N, 14.71%; H, 5.29%. Found: C, 48.62%; N, 13.95%; H, 5.58%. IR (KBr,  $\nu_{\max}$ /cm<sup>-1</sup>): 2927 (Pc–H), 1596 (Pc ring), 1255, 1017 (Ar–C–O), 1095 (C–N), 740 (Zn–N). MS (*m/z*): 1524 ([M + H]<sup>+</sup>).

#### 2.4.2. 2,9(10),16(17),23(24)-Tetra-{2-[4-(2-sulfoethyl)piperazin-1-yl]ethoxy}phthalocyanine zinc (**4a**)

The synthesis of **4a** was similar to **3a** in the presence of zinc acetate as metal salt, DMF/acetone = 1:1 (v/v) as eluent (1) and THF/benzene = 1:10 (v/v) as eluent (2) for purification. Compound **4a**: yield 27.2%. Elem. Anal. Calcd. for C<sub>64</sub>H<sub>80</sub>N<sub>16</sub>O<sub>16</sub>S<sub>4</sub>Zn: C, 50.47%; N, 14.71%; H, 5.29%. Found: C, 48.98%; N, 13.45%; H, 5.65%. IR (KBr,  $\nu_{\max}$ /cm<sup>-1</sup>): 2926 (Pc–H), 1608 (Pc ring), 1262, 1047 (Ar–C–O), 1092 (C–N), 747 (Zn–N). MS (*m/z*): 1524 ([M + H]<sup>+</sup>).

#### 2.4.3. 1,8(11),15(18),22(25)-Tetra-{2-[4-(2-sulfoethyl)piperazin-1-yl]ethoxy}phthalocyanine nickel (**3b**)

The synthesis of **3b** was similar to **3a** in the presence of anhydrous NiCl<sub>2</sub> as metal salt, DMF/CH<sub>3</sub>OH = 1:1 (v/v) as eluent (1) and ethanol/CH<sub>2</sub>Cl<sub>2</sub> = 10:1 (v/v) as eluent (2) for purification. Compound **3b**: yield 24.2%. Elem. Anal. Calcd. for C<sub>64</sub>H<sub>80</sub>N<sub>16</sub>O<sub>16</sub>S<sub>4</sub>Ni: C, 50.69%; N, 14.78%; H, 5.32%.

Found: C, 48.36%; N, 13.99%; H, 5.78%. IR (KBr,  $\nu_{\max}$ /cm<sup>-1</sup>): 2924 (Pc–H), 1607 (Pc ring), 1260, 1014 (Ar–C–O), 1092 (C–N), 740 (Ni–N). MS (*m/z*): 1518 ([M + 2H]<sup>+</sup>).

#### 2.4.4. 2,9(10),16(17),23(24)-Tetra-{2-[4-(2-sulfoethyl)piperazin-1-yl]ethoxy}phthalocyanine nickel (**4b**)

The synthesis of **4b** was similar to **3a** in the presence of anhydrous NiCl<sub>2</sub> as metal salt, DMF/acetone = 1:1 (v/v) as eluent (1) and acetone/CH<sub>3</sub>OH = 5:1 (v/v) as eluent (2) for purification. Compound **4b**: yield 23.5%. Elem. Anal. Calcd. for C<sub>64</sub>H<sub>80</sub>N<sub>16</sub>O<sub>16</sub>S<sub>4</sub>Ni: C, 50.69%; N, 14.78%; H, 5.32%. Found: C, 48.29%; N, 14.12%; H, 5.65%. IR (KBr,  $\nu_{\max}$ /cm<sup>-1</sup>): 2927 (Pc–H), 1606 (Pc ring), 1271, 1031 (Ar–C–O), 1095 (C–N), 751 (Ni–N). MS (*m/z*): 1516 (M<sup>+</sup>).

#### 2.4.5. 1,8(11),15(18),22(25)-Tetra-{2-[4-(2-sulfoethyl)piperazin-1-yl]ethoxy}phthalocyanine cobalt (**3c**)

The synthesis of **3c** was similar to **3a** in the presence of anhydrous CoCl<sub>2</sub> as metal salt, DMF/CH<sub>3</sub>CH<sub>2</sub>OH = 2:1 (v/v) as eluent (1) and methanol/CH<sub>2</sub>Cl<sub>2</sub> = 1:5 (v/v) as eluent (2) for purification. Compound **3c**: yield 27.6%. Elem. Anal. Calcd. for C<sub>64</sub>H<sub>80</sub>N<sub>16</sub>O<sub>16</sub>S<sub>4</sub>Co: C, 50.68%; N, 14.78%; H, 5.32%. Found: C, 48.72%; N, 13.66%; H, 5.54%. IR (KBr,  $\nu_{\max}$ /cm<sup>-1</sup>): 2928 (Pc–H), 1622 (Pc ring), 1279 (Ar–C–O), 1093 (C–N), 754 (Co–N). MS (*m/z*): 1517 (M<sup>+</sup>).

#### 2.4.6. 2,9(10),16(17),23(24)-Tetra-{2-[4-(2-sulfoethyl)piperazin-1-yl]ethoxy}phthalocyanine cobalt (**4c**)

The synthesis of **4c** was similar to **3a** in the presence of anhydrous CoCl<sub>2</sub> as metal salt, DMF/THF = 1:1 (v/v) as eluent

(1) and  $\text{C}_6\text{H}_5\text{CH}_3/\text{THF} = 5:1$  (v/v) as eluent (2) for purification. Compound **4c**: yield 25.3%. Elem. Anal. Calcd. for  $\text{C}_{64}\text{H}_{80}\text{N}_{16}\text{O}_{16}\text{S}_4\text{Co}$ : C, 50.68%; N, 14.78%; H, 5.32%. Found: C, 48.87%; N, 13.74%; H, 5.42%. IR (KBr,  $\nu_{\text{max}}/\text{cm}^{-1}$ ): 2927 (Pc–H), 1591 (Pc ring), 1245, 1013 (Ar–C–O), 1087 (C–N), 749 (Co–N). MS ( $m/z$ ): 1519 ( $[\text{M} + 2\text{H}]^+$ ).

#### 2.4.7. 1,8(11),15(18),22(25)-Tetra-[2-[4-(2-sulfoethyl)piperazin-1-yl]ethoxy]phthalocyanine copper (**3d**)

The synthesis of **3d** was similar to **3a** in the presence of CuCl as metal salt, DMF/ $\text{CH}_3\text{OH} = 1:1$  as eluent (1) and ethyl acetate/ $\text{CH}_3\text{OH} = 15:1$  (v/v) as eluent (2) for purification. Compound **3d**: yield 32.4%. Elem. Anal. Calcd. for  $\text{C}_{64}\text{H}_{80}\text{N}_{16}\text{O}_{16}\text{S}_4\text{Cu}$ : C, 50.53%; N, 14.73%; H, 5.30%. Found: C, 49.12%; N, 13.56%; H, 5.45%. IR (KBr,  $\nu_{\text{max}}/\text{cm}^{-1}$ ): 2933 (Pc–H), 1603 (Pc ring), 1267, 1037 (Ar–C–O), 1092 (C–N), 742 (Cu–N). MS ( $m/z$ ): 1522 ( $[\text{M} + \text{H}]^+$ ).

#### 2.4.8. 2,9(10),16(17),23(24)-Tetra-[2-[4-(2-sulfoethyl)piperazin-1-yl]ethoxy]phthalocyanine copper (**4d**)

The synthesis of **4d** was similar to **3a** in the presence of CuCl as metal salt, DMF/THF = 1:2 (v/v) as eluent (1) and  $\text{CH}_3\text{OH}/\text{CH}_2\text{Cl}_2 = 1:1$  (v/v) as eluent (2) for purification. Compound **4d**: yield 34.5%. Elem. Anal. Calcd. for  $\text{C}_{64}\text{H}_{80}\text{N}_{16}\text{O}_{16}\text{S}_4\text{Cu}$ : C, 50.53%; N, 14.73%; H, 5.30%. Found: C, 48.95%; N, 13.49%; H, 5.47%. IR (KBr,  $\nu_{\text{max}}/\text{cm}^{-1}$ ): 2935 (Pc–H), 1605 (Pc ring), 1251 (Ar–C–O), 1094 (C–N), 748 (Cu–N). MS ( $m/z$ ): 1521 ( $\text{M}^+$ ).

### 3. Results and discussion

#### 3.1. The UV–vis spectra of the title complexes in DMF solvent

The maximum absorption ( $\lambda_{\text{max}}$ ) of UV–vis spectra and corresponding molar extinction coefficient ( $\epsilon$ ) for all complexes dissolved in DMF are listed in Table 1.

Similar to other phthalocyanine compounds [9], the title complexes exhibited two characteristic absorption bands in their UV–vis spectra, namely Q-band and B-band, the former is in the visible region at ca. 600–750 nm, which may be attributed to the  $\pi-\pi^*$  transition ( $a_{1u}-e_g$ ) from HOMO to the LUMO of the conjugated  $\pi$ -bond system of phthalocyanine, and the latter is in the UV region at ca. 320–400 nm arising from the deeper  $\pi-\pi^*$  transitions ( $a_{2u}-e_g$ ). In addition, the absorptions of Q-band were observed as a band of high

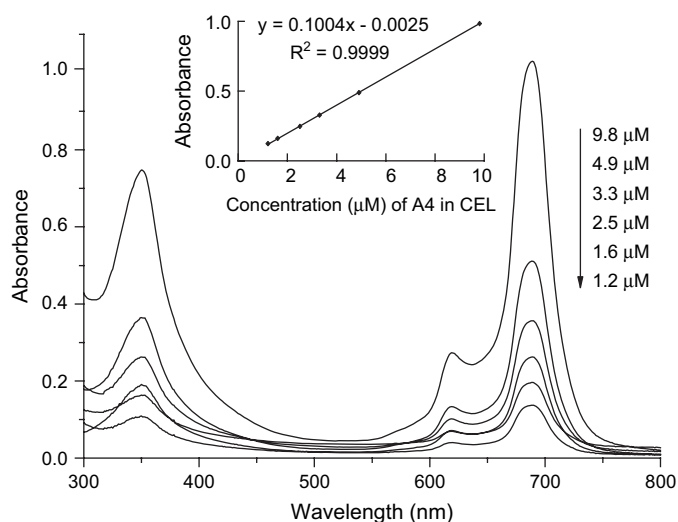


Fig. 2. Absorption spectra of **4a** in CEL solution. Inset: plot of concentration of **4a** in CEL vs. absorbance.

intensity usually also accompanying vibronic band at slightly higher energy side. All of complexes possess high molar extinction coefficient about  $10^5 \text{ L cm}^{-1} \text{ mol}^{-1}$ .

#### 3.2. The UV–vis spectra of the title complexes in aqueous media

All these complexes are able to disperse in 0.5% CEL (Cremophor EL) solution after these complexes were dissolved in DMF with concentrated solution. The absorption spectra of **4a** in CEL solution are shown in Fig. 2. These complexes showed very large molar extinction coefficient in CEL solution as listed in Table 2, which possessed the maximum absorption peak with a linear relationship between concentration and absorbance.

In case that water is used as solvent, these complexes show just a little solubility so that only can be examined by UV–vis spectra. But as these complexes existed as potassium salts, a considerably larger solubility is emerged. The typical curves of  $\beta$ -substituted potassium salt of the complexes in aqueous media are shown in Fig. 3. All absorption curves also show low aggregation of these complexes in aqueous media by the fact that the shoulder of the main absorption in the Q-band of the UV–vis disappears.

Table 1  
Maximum absorption and molar extinction coefficient of the title complexes in DMF

Complexes	<b>3a</b>	<b>3b</b>	<b>3c</b>	<b>3d</b>	<b>4a</b>	<b>4b</b>	<b>4c</b>	<b>4d</b>
Position of substituent	$\alpha$ -Position				$\beta$ -Position			
Central ion	$\text{Zn}^{2+}$	$\text{Ni}^{2+}$	$\text{Co}^{2+}$	$\text{Cu}^{2+}$	$\text{Zn}^{2+}$	$\text{Ni}^{2+}$	$\text{Co}^{2+}$	$\text{Cu}^{2+}$
Absorption in DMF, $\lambda_{\text{max}}$ (nm)	718	716	714	715	687	683	681	685
$\epsilon$ ( $\times 10^5 \text{ L cm}^{-1} \text{ mol}^{-1}$ )	1.46	1.32	1.59	1.57	0.80	1.04	0.93	1.23
B-band absorption (nm)	386	376	375	379	352	349	354	352

Table 2  
Maximum absorption and molar extinction coefficient of the title complexes in CEL solution

Complexes	3a	3b	3c	3d	4a	4b	4c	4d
Absorption in CEL, $\lambda_{\max}$ (nm)	717	715	714	715	689	682	681	684
$\epsilon$ ( $\times 10^5$ L cm $^{-1}$ mol $^{-1}$ )	1.57	0.92	1.35	1.23	1.00	1.08	1.05	1.33

### 3.3. Effects of peripherally substituted position and central ion on the Q-band

As those found in many phthalocyanines bearing alkoxy substituted moieties on the periphery [10], the Q-band absorption of the title complexes is shifted to lower energy side than that of unsubstituted phthalocyanines (ZnPc), due to the electron-donating character of alkoxy group. All of the  $\alpha$ -position substituted complexes **3a–d** show similar absorption positions of the Q-band at 713–718 nm in DMF solution together with two vibronic bands at 645–670 and 670–690 nm. All of the  $\beta$ -position substituted complexes **4a–d** show similar absorption positions of the Q-band at 680–687 nm in DMF solution together with two vibronic bands at 605–645 and 645–680 nm too. These mean that the influence on the red shift of  $\alpha$ -substituted complexes is larger than the other ones.

The red shift of Q-band in both  $\alpha$ - and  $\beta$ -substituted complexes has a similar order with different central ion as  $\text{Zn}^{2+} > \text{Cu}^{2+} > \text{Ni}^{2+} > \text{Co}^{2+}$ , which obviously is caused by the difference of 3d electronic numbers in LUMO.

### 3.4. Effect of solvent on electronic absorption spectra

Table 3 shows Q-band red shift of **3a** in various solvents. In general, as the refractive index of the solvent increased, the red shift of Q-band increased. The electronic absorption spectra of **3a** in the various solvents were analyzed by using the method described originally by Bayliss [11]. The plot of  $F = (n^2 - 1)/(2n^2 + 1)$  (where  $n$  is the refractive index) vs. the red shift in

the Q-band was shown in Fig. 4. The linear nature of the plot suggests that the red shift in the Q-band is mainly a result of solvation rather than coordination of solvent molecule. As a strong coordination solvent such as DMF is used, the red shift is smaller than that in a weaker coordination solvent such as dichloromethane, confirming that coordination of the solvent molecule does not play a significant role in the red shift. The relationship between the maximum absorption wavelength and the  $F$  factor of the solvent can be evaluated by Eq. (1):

$$\lambda_{\max}(\text{nm}) = 0.0038F + 0.0156 \quad (1)$$

with  $R^2 = 0.9192$ .

### 3.5. Fluorescence emission spectra and quantum yields

The fluorescence emission spectra and quantum yields were determined by using ZnPc ( $\Phi_f = 0.32$  in DMF [12]) as standard substance. For the excitation of the complexes, two wavelengths were chosen, one at 610 nm and the other at 640 nm. For the  $\beta$ -substituted complexes the irradiation beam with 610 nm was chosen as usually used in literature [13], while for the  $\alpha$ -substituted complexes the irradiation beam with 640 nm was used because their absorptions were too weak in 610 nm region. Quantum yields of all complexes are shown in Table 4. The calculation is performed by Eq. (2):

$$\Phi_f = 0.32 \frac{A_{\text{ZnPc}} S}{S_{\text{ZnPc}} A} \quad (2)$$

where  $\Phi_f$  represents the fluorescence quantum yield of the complexes,  $A_{\text{ZnPc}}$  represents the absorbance of ZnPc at 610 nm or 640 nm,  $S_{\text{ZnPc}}$  represents emission area of ZnPc,  $A$  represents the absorbance of the complexes,  $S$  represents emission area of the complexes.

Table 3  
Q-band red shifts of **3a** in various solvents on comparison with ZnPc ( $\lambda_{\max} = 670$  nm)

Solvent	Dipole moment, $\mu$	Refractive index, $n_D$	Q-Band, $\lambda_{\max}$ (nm)	Red shift (nm)
Acetone	2.88	1.359	712.5	42.5
Methanol	1.71	1.329	713.6	43.6
Ethyl acetate	1.78	1.372	714.5	44.5
Ethanol	1.69	1.361	715.0	45.0
THF	1.75	1.406	717.3	47.3
DMF	3.82	1.430	718.1	48.1
$\text{CH}_2\text{Cl}_2$	1.36	1.445	721.6	51.6
Chloroform	1.90	1.438	721.7	51.7

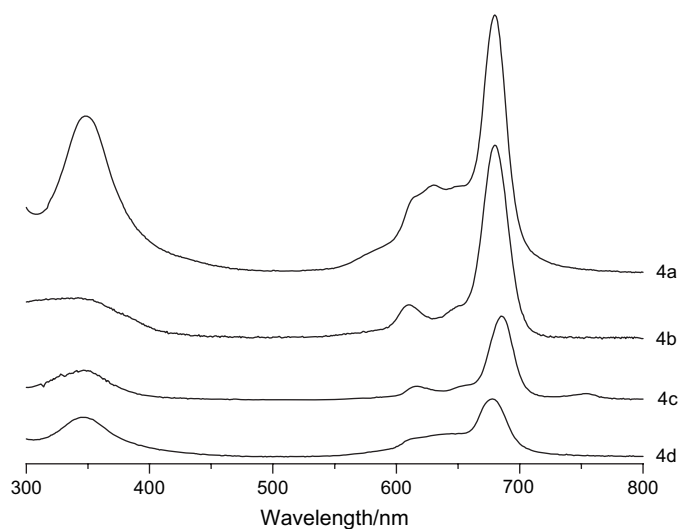


Fig. 3. Absorption spectra of  $\beta$ -substituted potassium salts of the complexes in aqueous media.



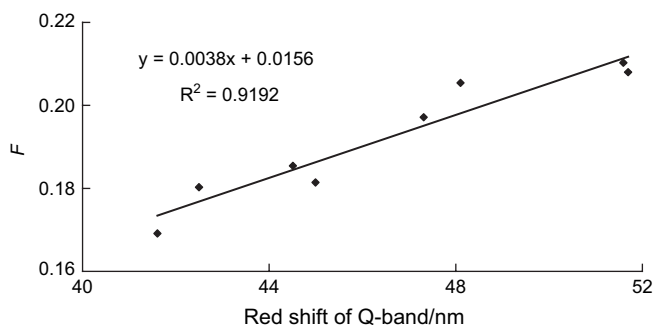


Fig. 4. Plot of red shift of Q-band vs.  $F$  (for **3a**); (1) acetone, (2)  $\text{CH}_3\text{OH}$ , (3) ethyl acetate, (4) ethanol, (5) THF, (6) DMF, (7)  $\text{CH}_2\text{Cl}_2$ , and (8) chloroform.

It can be seen from Table 4 that upon excitation at 610 nm, the  $\beta$ -substituted complexes **4a–d** showed a strong fluorescence emission at ca. 690 nm with a Stock's shift of 3–11 nm and a fluorescence quantum yield ( $\Phi_f$ ) of 0.01–0.18. While for the  $\alpha$ -substituted complexes, only complex **3a** showed a strong fluorescence emission at 725 nm with a Stock's shift of 9 nm and a fluorescence quantum yield ( $\Phi_f$ ) of 0.08 upon excitation at 640 nm.

### 3.6. Rate of singlet oxygen yields

The procedure for the determination of singlet oxygen yield under irradiation was as follows: DMSO solutions containing phthalocyanine complexes ( $1 \times 10^{-5}$  mol/L<sup>3</sup>) and 1,3-diphenyl-benzoisofuran (DPBF,  $3 \times 10^{-5}$  mol/L) were prepared in the dark. Two milliliters of such solution in cuvette was bubbled by oxygen gas continuously and irradiated by 670 nm point laser concurrently. Under the irradiation of laser beam, the phthalocyanine complexes produce singlet oxygen, then DPBF is acted as capturer of singlet oxygen so as to be decomposed itself. Meanwhile the characteristic absorption at 417 nm of DPBF was decreased, the concentration of DPBF was calculated by Lambert–Beer Law. The time decay of absorbance on 417 nm for each phthalocyanine complex is true to first-order reaction. The rate of singlet oxygen yields is listed in Table 5, which is calculated by following Eq. (3):

$$\ln \frac{[\text{DPBF}]_0}{[\text{DPBF}]_t} = kt \quad (3)$$

where  $[\text{DPBF}]_0$  and  $[\text{DPBF}]_t$  in mol/L are the concentrations of DPBF prior and after irradiation, respectively. Values of  $k$  are the rate of singlet oxygen yields and  $t$  is the time of irradiation.

Table 4  
Stock's shift and quantum yields of the complexes

Product	<b>3a</b>	<b>3b</b>	<b>3c</b>	<b>3d</b>	<b>4a</b>	<b>4b</b>	<b>4c</b>	<b>4d</b>
$\lambda_{\text{ex}}$ (nm)	640	—	—	—	610	—	—	—
Maximum $\lambda_{\text{flu}}$ (nm)	725	—	—	—	697	694	690	688
Stock's Shift (nm)	9	—	—	—	10	11	9	3
$\Phi_f$	0.08	$\approx 0$	$\approx 0$	$\approx 0$	0.18	0.04	0.01	0.01

Table 5  
Rate of singlet oxygen yields of all complexes

Product	<b>3a</b>	<b>3b</b>	<b>3c</b>	<b>3d</b>	<b>4a</b>	<b>4b</b>	<b>4c</b>	<b>4d</b>
Central ion	$\text{Zn}^{2+}$	$\text{Ni}^{2+}$	$\text{Co}^{2+}$	$\text{Cu}^{2+}$	$\text{Zn}^{2+}$	$\text{Ni}^{2+}$	$\text{Co}^{2+}$	$\text{Cu}^{2+}$
Electronic configuration	$3d^{10}$	$3d^8$	$3d^7$	$3d^9$	$3d^{10}$	$3d^8$	$3d^7$	$3d^9$
$k$ ( $\text{min}^{-1}$ )	2.8	0.40	0.26	0.39	1.0	0.45	0.37	0.42

It can be seen from Table 5 that the complexes with zinc as central ion have the largest singlet oxygen yield while the singlet oxygen yield of complexes with other central ions was considerably weaker. This means that the complexes with closed shell electronic structure as central ion is beneficial to singlet oxygen production as shown in literature [14].

### Acknowledgments

This study was supported by National Natural Science Foundation of China (Grant No. 20201005) and Natural Science Foundation of Fujian (Grant No. E0513011).

### References

- [1] McKeown NB. Phthalocyanine materials synthesis, structure and function. London: Cambridge University Press; 1998.
- [2] Marcus SL. Photodynamic therapy of human cancer. Proceedings of the IEEE 1992;80(6):869–89.
- [3] Dirk DV, Huwyler J, Eberle A, et al. Targeting of the photocytotoxic compound AlPcS4 to Hela cells by transferrin conjugated PEG-liposomes. Canada International Journal of Cancer 2002;101:78–85.
- [4] Stranadko EF, Skobelkin OK, Litvin GT, et al. Photodynamic therapy of human malignant tumors: a comparative study between Photogem and tetrasulfonated aluminium phthalocyanine. Proceedings of the SPIE 1996;2625:440–8.
- [5] Li YS, Kenney EM. Methods of syntheses of phthalocyanine compounds. The United States Patent, 5763602.
- [6] Huang JL, Chen NS, Liu ES, et al. Invention Patents of China, Patent No: ZL96117137.5, Opening No: CN1053906C RPC.
- [7] Wei JH, Luo XX. The bioeffects of HEPEs. The Foreign Medical Physiology and Pathematology 1997;17(3):271–3 [in Chinese].
- [8] Shi Y. In: Perrin DD, Arovedo WLF, Perrin DR, editors. The method of purification of laboratory chemical agents. Beijing: Chemical Industry Press; 1997.
- [9] Kobayashi N. Phthalocyanines. Current Opinion in Solid State and Materials Science 1999;4:345–53.
- [10] Hiromi S, Olga T, Gunter S, et al. Differently substituted phthalocyanines: comparison of calculated energy levels, singlet oxygen quantum yields, photo-oxidative stabilities, photocatalytic and catalytic activities. Journal of Photochemistry and Photobiology A: Chemistry 2006; 184:50–7.
- [11] Bayliss NS. The effect of the electrostatic polarization of the solvent on electronic absorption spectra in solution. Journal of Chemical Physics 1950;18(3):292–6.
- [12] Zhang XF, Xu HJ. Influence of halogenation and aggregation on photosensitizing properties of zinc phthalocyanine (ZnPc). Journal of Chemical Society Faraday Transition 1993;89(18):3347–51.
- [13] Abimbola O, David M, Tebello N. Solvent effects on the photochemical and fluorescence properties of zinc phthalocyanine derivatives. Journal of Molecular Structure 2003;650:131–40.
- [14] Tayyaba H, Anne CEM, Bernard O. In: Robert CB, Donald WK, Raphael EP, et al., editors. Cancer medicine. London: BC Decker Inc; 2000. p. 489–501.